

Supplementary Materials for **Analysis of the bystander effect in cone photoreceptors via a guided neural network platform**

Yuan Ma, Xin Han, Ricardo Bessa de Castro, Pengchao Zhang, Kai Zhang, Zhongbo Hu, Lidong Qin

Published 9 May 2018, *Sci. Adv.* **4**, eaas9274 (2018)

DOI: 10.1126/sciadv.aas9274

The PDF file includes:

- fig. S1. Optimization of the parameters and conditions for high-efficiency 661W cell loading.
- fig. S2. A schematic shows the microwell BME-coating process on the NN-Chip.
- fig. S3. ROS production, mmp measurements, and SYTOX function test in the blue light-treated 661W cells.
- fig. S4. Representative immunostaining images of S-opsin from 0 to 18 hours under blue light irradiation.
- fig. S5. Existence of tight junctions in synapses and function validation of the SYTOX.
- fig. S6. Apoptotic cells were quantified with or without adjacent apoptotic cells ($n = 10$).
- fig. S7. Generation and verification of Cx36-KO 661W cells.
- fig. S8. Calibration of the microinjection volume.
- Legends for movies S1 to S4

Other Supplementary Material for this manuscript includes the following:

(available at advances.sciencemag.org/cgi/content/full/4/5/eaas9274/DC1)

- movie S1 (.avi format). Operation of NN-Chip.
- movie S2 (.mp4 format). Three-dimensional structural view of 661W cells cultured onto NN-Chip after 6 hours.
- movie S3 (.mov format). Time lapse of the gap junction-mediated bystander killing effect in the 661W cells.
- movie S4 (.mov format). Apoptosis propagation from single cell.

Supplementary Materials

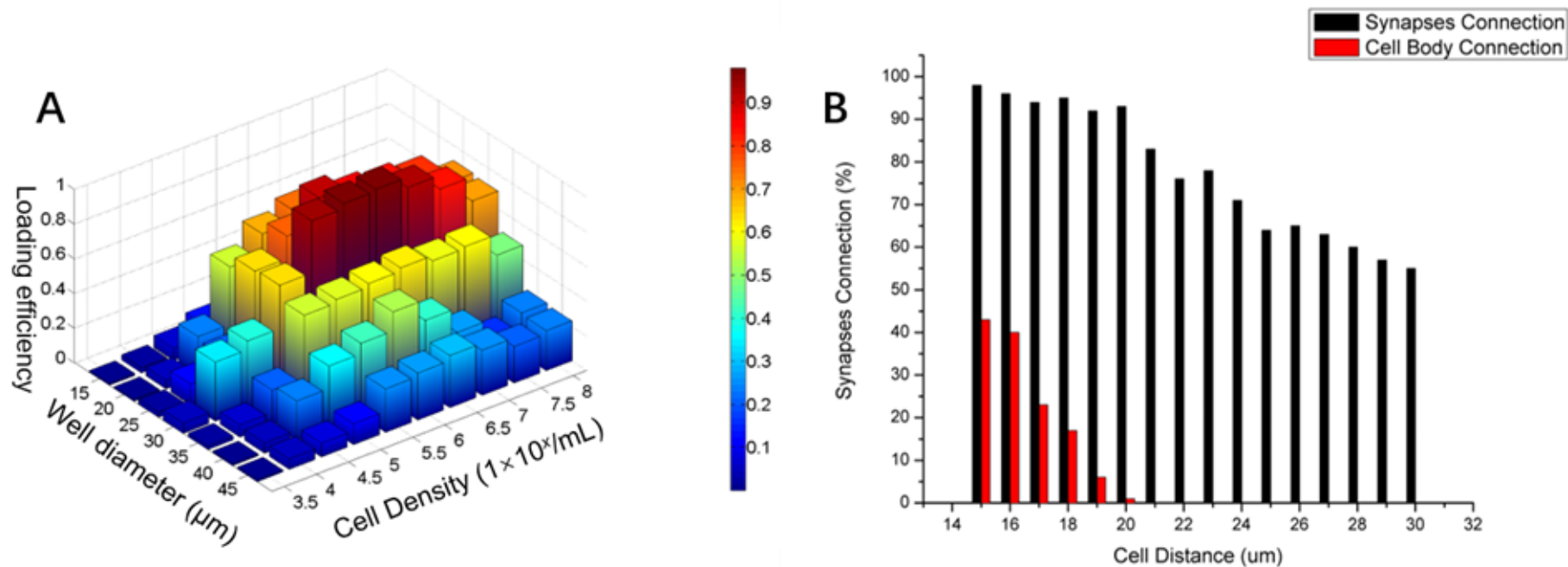


fig. S1. Optimization of the parameters and conditions for high-efficiency 661W cell loading. (A) The cell-loading efficiency was tested at different cell concentrations and microwell diameters. The highest efficiency is approximately 95%, which occurred around cell concentration of $2 \times 10^6/\text{mL}$ and a 20- μm microwell diameter. (B) The synapse-connection efficiency was tested at different cell distances (channel lengths). The optimal cell distance was 20 μm , which showed low cell-body, and high synapse connection efficiency ($n = 50$).

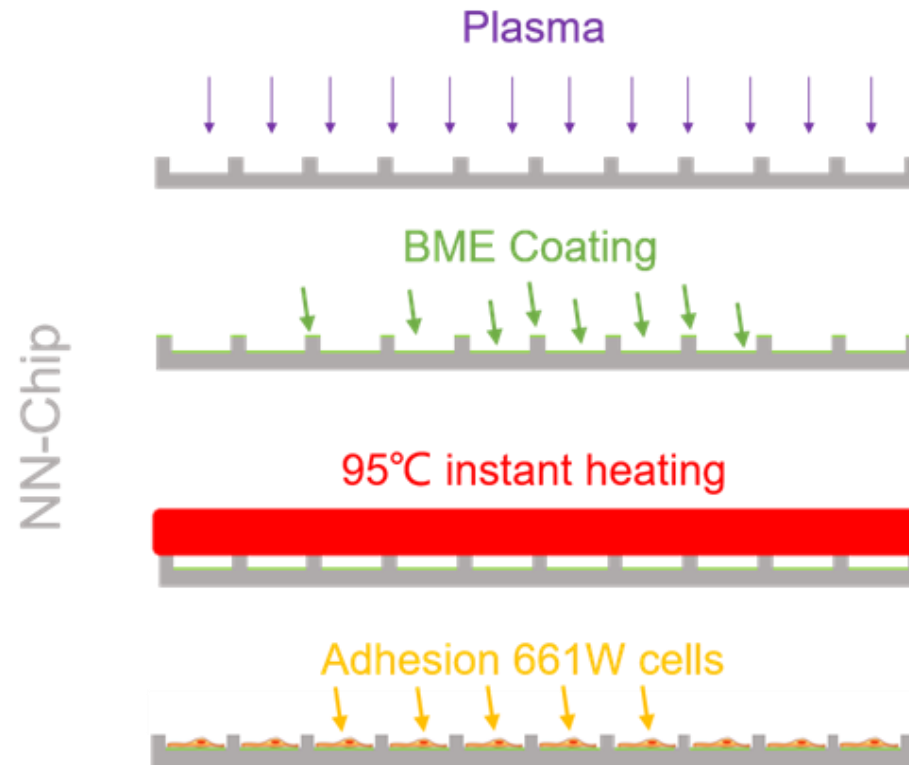


fig. S2. A schematic shows the microwell BME-coating process on the NN-Chip. First, PDMS was treated with plasma to create a hydrophilic surface. Second, BME was applied to the entire NN-chip surface, and then rapidly heat the surface at 95°C by a hot plate to denature the coated BME in contacted area. The denatured BME was then removed by tapes. After treatment, the cultured cells should be unable to migrate outside of the wells. See Materials and Methods for more details.

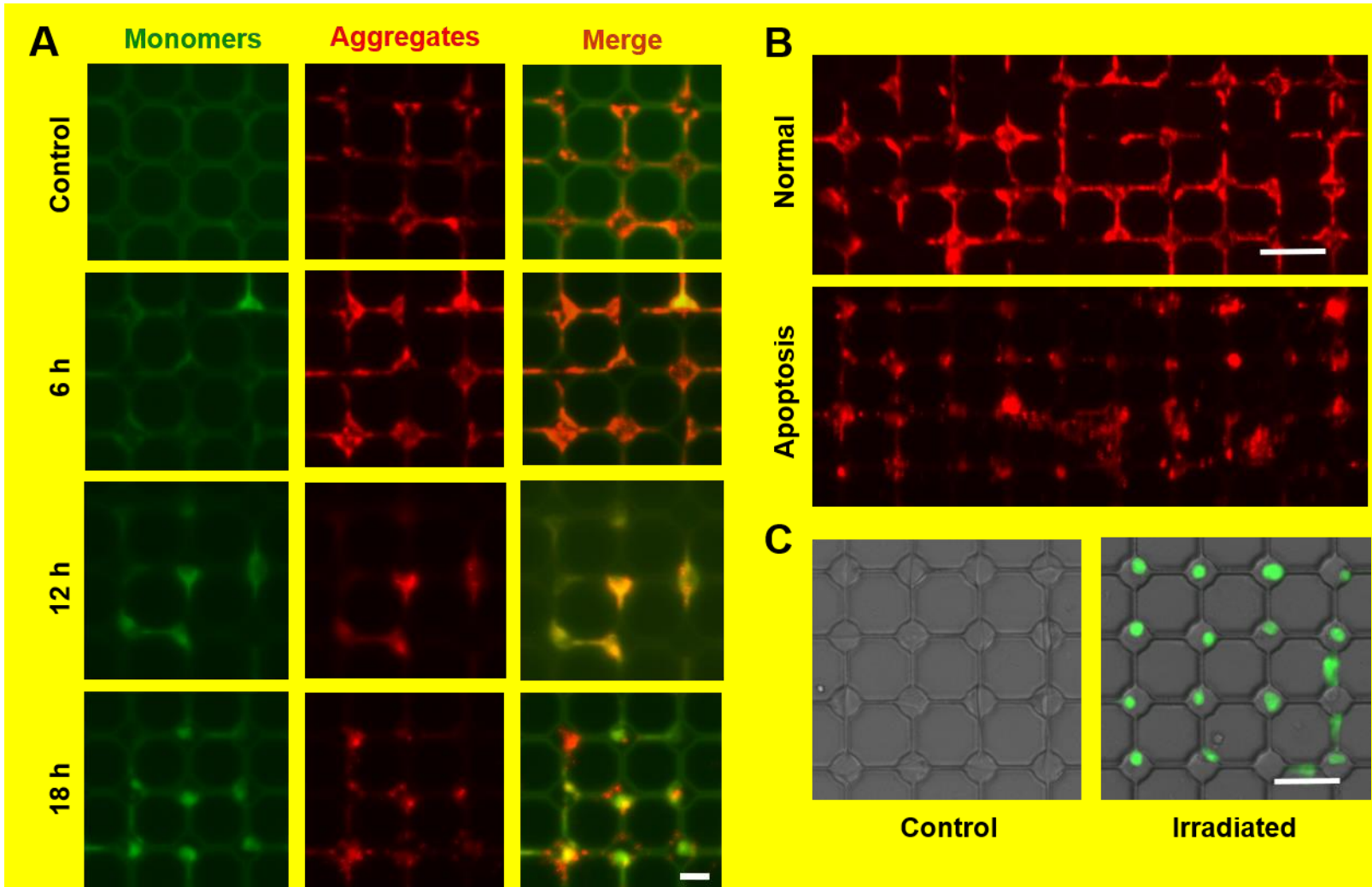


fig. S3. ROS production, mmp measurements, and SYTOX function test in the blue light–treated 661W cells. (A) Representative images show JC-1-stained 661W cells after blue light irradiation for varying times. Scale bar: 20 μm . **(B)** Mitochondria distribution in healthy and apoptotic 661W cells on the NN-Chip after stained by JC-1 mitochondrial membrane potential assay. In the apoptotic cells, there are relatively few mitochondria in the dendritic synapses, and the mitochondria appear randomly dispersed accompanying the cells degeneration. Scale bar: 40 μm **(C)** Representative images show that the control and irradiated cells were incubated with SYTOX-Green for 1 h after blue light irradiation only on one group for 18 h. Scale bar: 40 μm

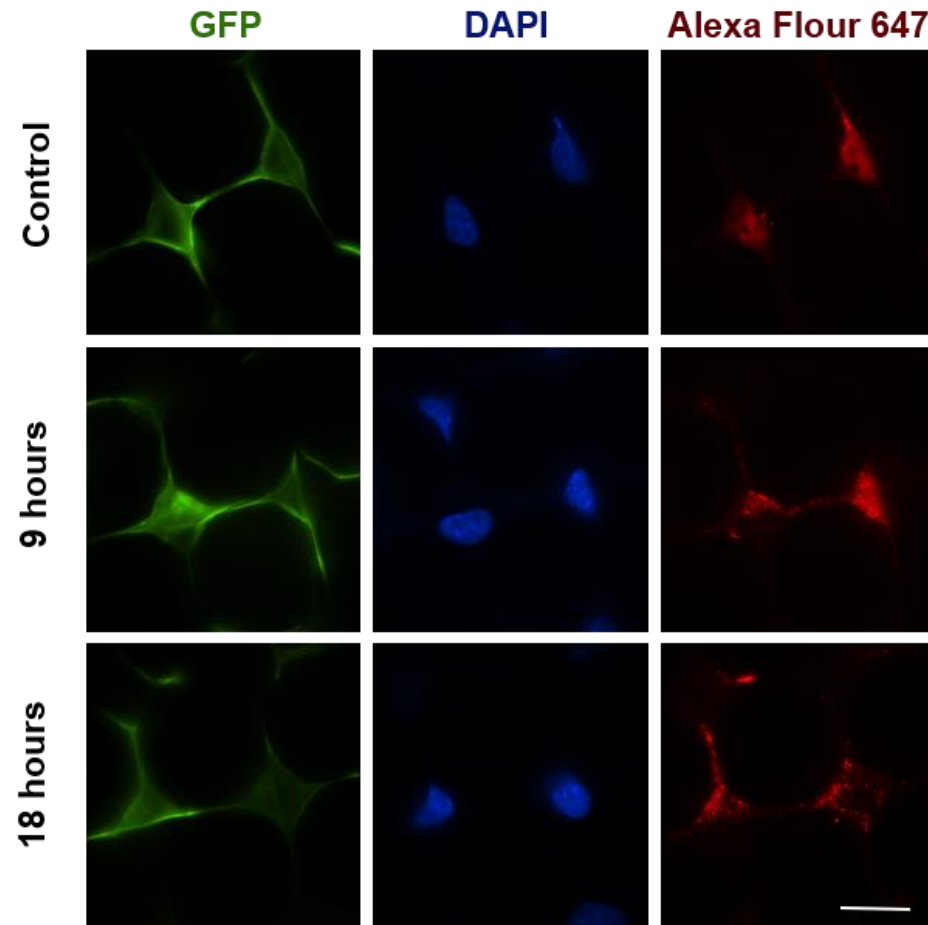


fig. S4. Representative immunostaining images of S-opsin from 0 to 18 hours under blue light irradiation. Actin (GFP), nuclei (DAPI) and S-opsin (Alexa Fluor 647) were stained in the images. Scale bar: 20 μm

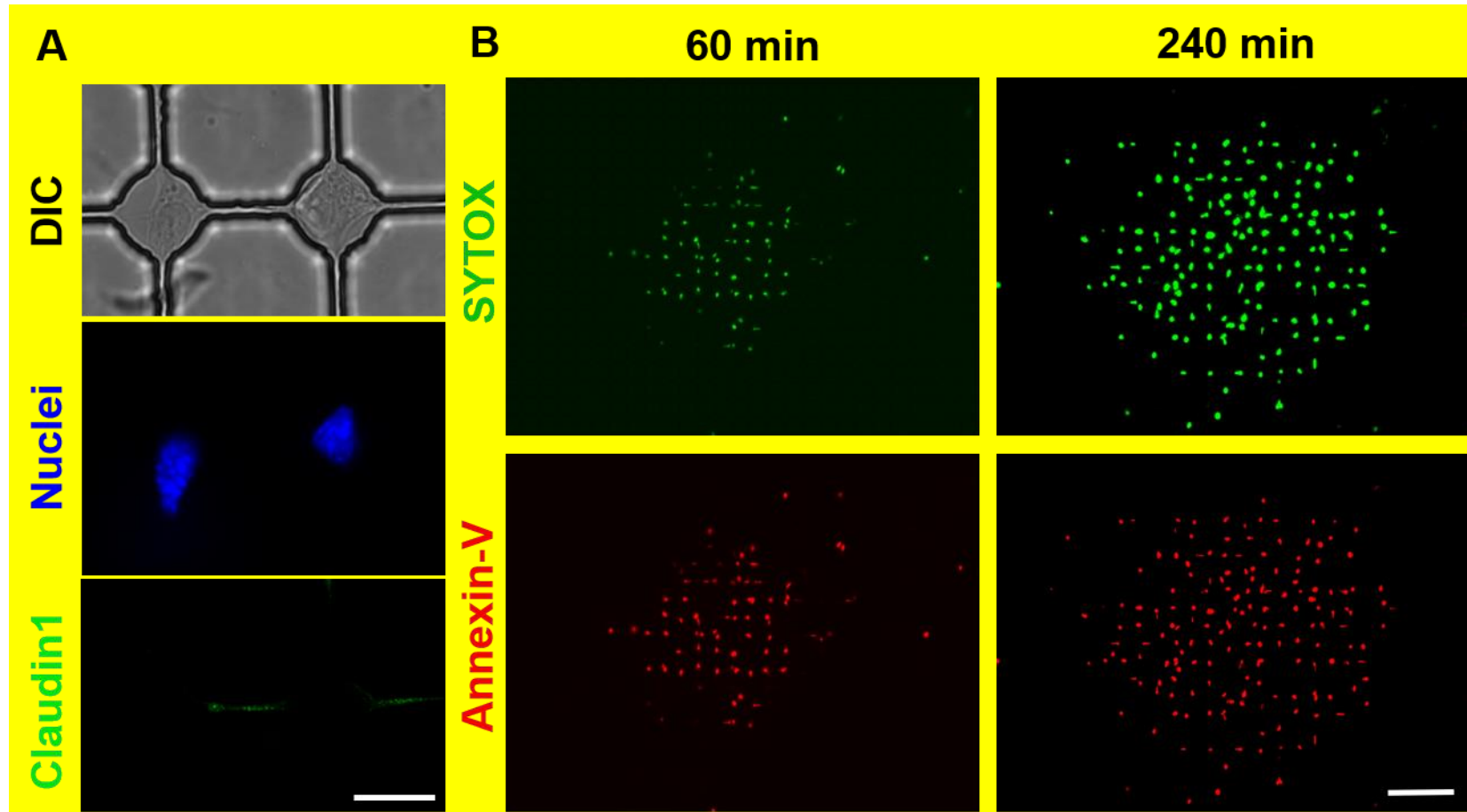


fig. S5. Existence of tight junctions in synapses and function validation of the SYTOX. (A) Representative images show the existence of tight junctions in the connected synapses between two neighboring 661W cells while culturing on the NN-Chip. Scale bar: 20 μm (B) Images show the 661W staining results that were incubated with SYTOX (green) and Annexin-V (red) for 60 min and 240 min after blue light irradiation. SYTOX can diffuse across the synapse channels, whereas Annexin-V (a membrane protein stain) cannot. These same staining results confirming that SYTOX is a reliable staining apoptotic cells indicator throughout the experiments. Scale bar: 200 μm

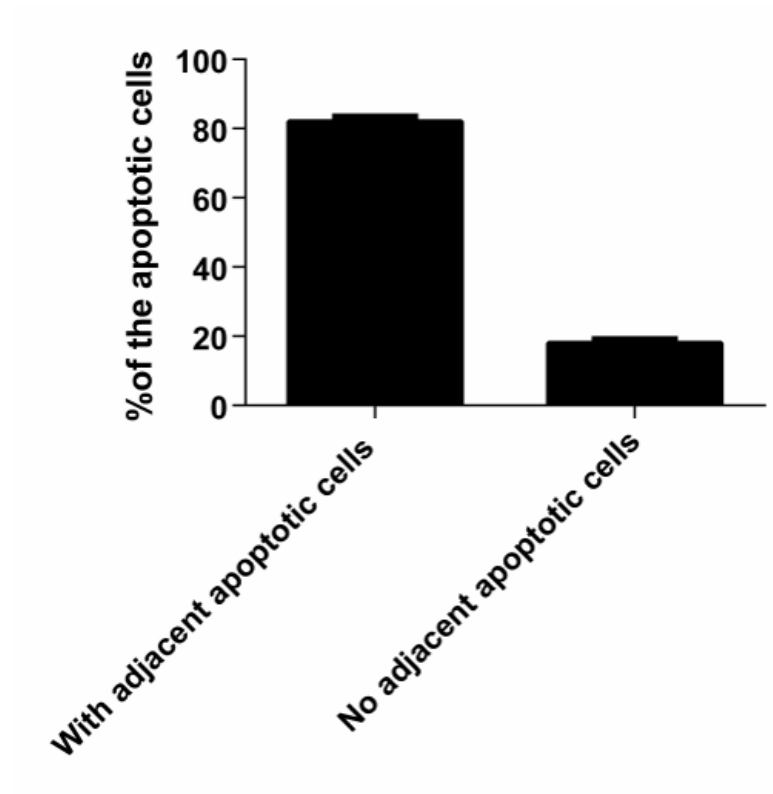


fig. S6. Apoptotic cells were quantified with or without adjacent apoptotic cells ($n = 10$).

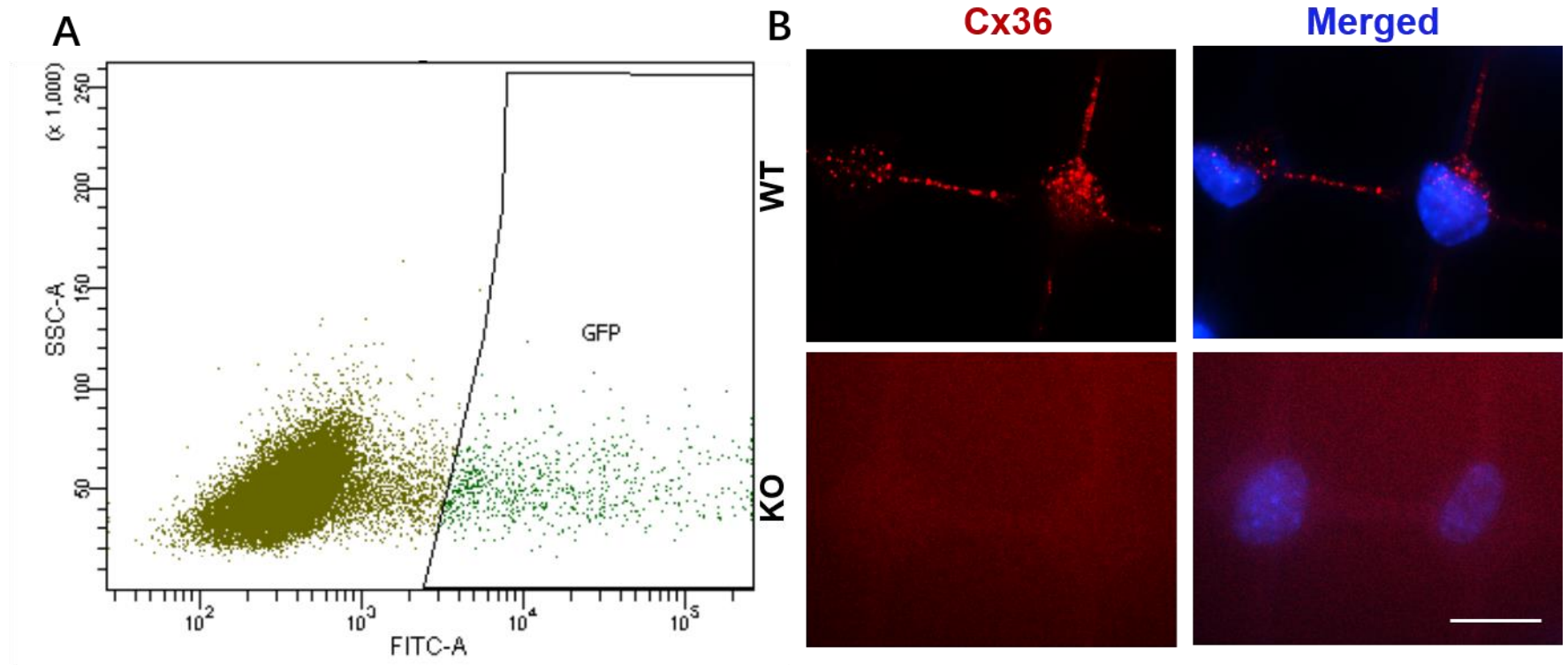


fig. S7. Generation and verification of Cx36-KO 661W cells. (A) A dot plot shows the GFP-positive 661W cells that were sorted by fluorescence-activated cell sorting after transfection with the GFP-labeled, CRISPR-Cas9-Cx36-KO plasmid. (B) Representative immunostained images show loss of Cx36 (red) in the KO cells compared with the wild-type (WT) cells. Nuclei were stained with DAPI. Scale bar: 20 μm

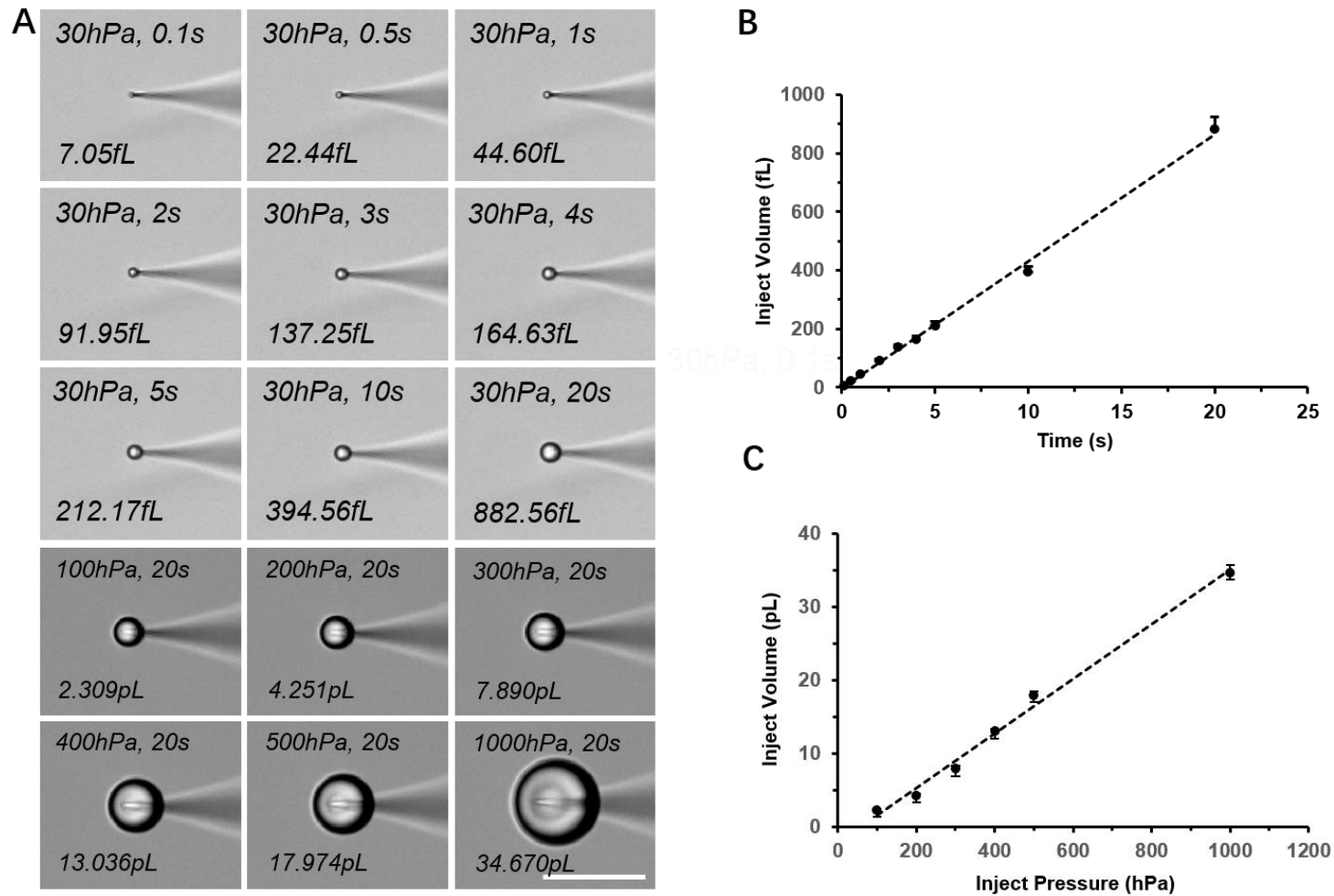


fig. S8. Calibration of the microinjection volume. (A) Water droplets were dispensed in mineral oil after injection. Scale bar: 10 μm (B) A graph shows linearity of the injection volume versus the injection time. (C) A graph shows linearity of the injection volume versus the injection pressure. The error bars in both graphs indicate the SD of five independent experiments. The compensation pressure was 270 hPa.

movie S1. Operation of NN-Chip.

movie S2. Three-dimensional structural view of 661W cells cultured onto NN-Chip after 6 hours.

movie S3. Time lapse of the gap junction–mediated bystander killing effect in the 661W cells. (1) Apoptosis spreading results of control group from 0 to 24 h. (2) Apoptosis spreading results of octanol treated group from 0 to 24 h.

movie S4. Apoptosis propagation from single cell.